WATANABE, T., HAYASHI, M., HAYASHI, S., FUKUYAMA, H. and NAGATA, K. Solid-state $^{19}F$ NMR on CaO-SiO$_2$-CaF2 glasses. *VII International Conference on Molten Slags Fluxes and Salts,* The South African Institute of Mining and Metallurgy, 2004.

# Solid-state $^{19}F$ NMR on CaO-SiO$_2$-CaF$_2$ glasses

T. WATANABE*, M. HAYASHI†, S. HAYASHI‡, H. FUKUYAMA* and K. NAGATA*
**Department of Chemistry and Materials Science Tokyo Institute of Technology, Tokyo, Japan*
*†Department of Materials Science and Engineering, Royal Institute of Technology, Stockholm, Sweden*
*‡Institute for Materials and Chemical Process, National Institute of Advanced Industrial Science and Technology, Ibaraki, Japan*

Chemical states of fluorine in CaO-SiO$_2$-CaF$_2$ glasses in a composition range of CaO/SiO$_2$ = 0.5–1.3 and 5–25 mol%CaF$_2$ have been investigated by $^{19}F$ solid-state NMR with and without MAS. The isotropic chemical shifts of the glasses are close to those of cuspidine crystal (59.4 and 64.3 ppm with respect to $C_6F_6$) and CaF$_2$ crystal (58.6 ppm). The fluoride ions are coordinated with four or less than four calcium ions in this composition range. The chemical shifts move to the lower frequency with an increase in the CaF$_2$ content, whereas those are not affected by the CaO/SiO$_2$ ratio. The ionic distance between calcium and fluoride ions increases with an increase in the CaF$_2$ content. The chemical state of fluorine is not disturbed by the degree of polymerization of the silicate network.

Comparing the MAS and static NMR spectra, the second moment attributed to $^{19}F$-$^{19}F$ dipole-dipole interaction has been estimated. The values of the glasses range over 3.1–7.3×10$^7$ Hz$^2$ and those are larger than the calculated value of cuspidine crystal. This indicates that fluoride ions form Ca-F clusters in the glasses and that the size of clusters increases with increasing the CaF$_2$ content.

Keywords: chemical state of fluoride ion, CaO-SiO$_2$-CaF$_2$ glass, solid state $^{19}F$ NMR spectroscopy

## Introduction

It is widely known that addition of CaF$_2$ lowers both viscosity and liquidus temperature of slag. CaF$_2$ has been used for steelmaking slags to promote the melting of CaO and slag/metal reaction because of its strong fluxing power. CaF$_2$ has also been used for mold fluxes of continuous casting of steel and is also an indispensable compound for crystallizing of cuspidine (3CaO•2SiO$_2$•CaF$_2$) in the flux films. In the initial solidification of steel, cuspidine crystals promote the mild cooling of the steel shell to decrease the number of longitudinal cracks.[1]. It is necessary for controlling the crystallization to determine the stable area of cuspidine and elucidate the mechanism of crystallization. The authors reported the phase diagram of the CaO-SiO$_2$-CaF$_2$ system and the stable area of cuspidine[2]. The mechanism of crystallization and physicochemical properties strongly depend on the structure.

There are many reports intended to elucidate the mechanism improving the properties of slags containing CaF$_2$ by means of thermochemical and physicochemical approaches and spectroscopy[3-14]. Some researchers provided an explanation that CaF$_2$ shows two different behaviours; in basic slag, CaF$_2$ dissolves into Ca$^{2+}$ and F$^-$ ions, which does not contribute to breaking the silicate network, while in acidic slag, fluorine atoms are bonded to silicon and calcium ions are coordinated with non-bridging oxygen.[6-8]. However, the latter model has not been generally accepted because of some conflicting reports[9-12].

$^{19}F$ nuclear magnetic resonance (NMR) spectroscopy is one of the most useful means of determining the coordination number and the coordination geometry, though there are few reports using $^{19}F$ NMR in this system except the reports of Stebbins *et al.*[13,14]. In this study, chemical states of fluoride ion in CaO-SiO$_2$-CaF$_2$ glasses have been investigated using $^{19}F$ NMR with and without magic angle spinning (MAS).

## Experimental procedure

### Sample preparation

Reagent grade powders of CaCO$_3$ (99.5 mass%), SiO$_2$ (99.9 mass%) and CaF$_2$ (99.8 mass%) were used. CaO powder was obtained by firing CaCO$_3$ at 1573 K for 43.2 ks in a dried argon atmosphere. CaO, SiO$_2$ and CaF$_2$ powders were weighed at various initial compositions and mixed in an alumina mortar. Three series of samples were prepared as follows:

Series I: $(100-x)/2$CaO-$(100-x)/2$SiO$_2$-$x$CaF$_2$
($x$= 5, 10, 15, 20, 25)
Series II: $(100-x)/3$CaO-$2(100-x)/3$SiO$_2$-$x$CaF$_2$
($x$= 5, 10, 15, 20, 25)
Series III: $x$CaO-$y$SiO$_2$-15CaF$_2$
($x/y$= 0.7, 0.9, 1.0, 1.1, 1.3)

There were a few reports that fluorine predominantly bonds with silicon for the glasses less than 10 mol% CaF$_2$[7,8]. Series I and II were prepared in order to evaluate the CaF$_2$-composition dependence of the chemical states of fluoride ions in basic and acidic glasses. Some reports said that CaF$_2$ leads to depolymerization of the silicate network by forming Si-F bonds in acidic glasses[6, 8]. Series III were

**Table I**
**Sample compositions and chemical shifts for $^{19}F$ in MAS NMR**

| | composition (mass%) | | | composition (mol%) | | | density | chemical | Series | | |
|---|---|---|---|---|---|---|---|---|---|---|---|
| | CaO | $SiO_2$ | $CaF_2$ | CaO | $SiO_2$ | $CaF_2$ | (gcm$^{-3}$) | shift (ppm)* | I | II | III |
| glass1 | 41.88 | 40.50 | 17.62 | 45.36 | 40.93 | 13.71 | 3.448 | 72 | _ | _ | |
| glass2 | 45.58 | 37.31 | 17.11 | 49.17 | 37.57 | 13.26 | 3.335 | 71 | | | _ |
| glass3 | 35.43 | 47.28 | 17.29 | 38.52 | 47.97 | 13.50 | 2.903 | 67 | | | _ |
| glass4 | 38.80 | 41.87 | 19.33 | 42.28 | 42.59 | 15.13 | 3.117 | 72 | | | _ |
| glass5 | 36.38 | 36.89 | 26.73 | 40.42 | 38.25 | 21.33 | 3.008 | 70 | _ | | |
| glass6 | 44.91 | 43.29 | 11.80 | 47.88 | 43.08 | 9.04 | 2.945 | 75 | _ | | |
| glass7 | 43.89 | 41.33 | 14.78 | 47.16 | 41.44 | 11.40 | 2.966 | 72 | _ | | |
| glass8 | 47.17 | 46.72 | 6.11 | 49.57 | 45.82 | 4.61 | 2.956 | 78 | _ | | |
| glass9 | 32.78 | 61.18 | 6.04 | 34.79 | 60.61 | 4.60 | 2.868 | 72 | | _ | |
| glass10 | 33.25 | 65.40 | 3.07 | 34.46 | 63.26 | 2.29 | 2.768 | 75 | | _ | |
| glass11 | 34.23 | 54.18 | 11.59 | 36.76 | 54.30 | 8.94 | 2.833 | 72 | | _ | |
| glass12 | 31.78 | 49.50 | 18.72 | 34.76 | 50.53 | 14.71 | 2.831 | 75 | | _ | _ |
| glass13 | 29.37 | 45.87 | 24.75 | 32.65 | 47.59 | 19.76 | 2.840 | 67 | | _ | |

*: All chemical shifts have been comverted to the $^{19}F$ scale with $\delta(C_6F_6)=0$

prepared to evaluate the effect of basicity on the chemical states of fluoride ions. 0.2 mass% CoO was added to the sample powder to accelerate spin-lattice relaxation. About 20 g of these mixtures was melted in platinum crucibles at 1723–1823 K in a dried argon atmosphere for 1.8 ks. Each sample was quenched by pressing with two copper plates. It was confirmed that the samples were amorphous by X-ray diffractometry (XRD) and the compositions were determined by quantitative analysis using an electron probe microanalyzer (EPMA). The fluorine concentration in Å$^{-3}$ was estimated from the sample composition and the density determined by Archimedean method with water.

Fluorite ($CaF_2$) and cuspidine ($3CaO\bullet 2SiO_2\bullet CaF_2$) powders, which was crystallized from the melt of a stoichiometric mixture of CaO, $SiO_2$ and $CaF_2$ with 0.2 mass% CoO in a platinum hermetic capsule, were measured as crystalline model compounds.

### $^{19}F$ solid state NMR spectroscopy

$^{19}F$ NMR spectra were measured at room temperature by a Bruker ASX200WB spectrometer, the magnetic field of which was 4.7 T. Larmor frequency of $^{19}F$ was 188.28 MHz. The spectra were traced under MAS and static conditions.

### *Magic angle spinning NMR*

The sample powders were packed into a ϕ4.0 mm MAS rotor. The spinning rates were in the range between 8 and 12 kHz. The ordinary single-pulse sequence was used every 40 s and 32 free induction decay (FID) signals were accumulated. A background signals from F in the rotor cap materials was subtracted after matched experiments on an empty rotor. Spectra were referenced to $KPF_6$ powder, which has signals at 94.98 and 91.06 ppm relative to the standard of $C_6F_6$. The NMR spectra were fitted by the following Gaussian curves:

$$F(\nu) = A_{MAS}\left\{ \begin{array}{l} \dfrac{1}{\beta_{MAS}\sqrt{2\pi}}\exp\left[-\dfrac{(\nu-\nu_0)^2}{2\beta_{MAS}^2}\right] \\ +\displaystyle\sum_{i=1}^{2}\dfrac{B_{i,\,MAS}}{\beta_{MAS}\sqrt{2\pi}}\exp\left[-\dfrac{(\nu-\nu_{o,\,MAS}\pm\Delta_i)^2}{2\beta_{MAS}^2}\right] \end{array} \right\} + C_{MAS} \qquad [1]$$

where $\beta_{MAS}$ is the width between the center and the inflection point of the Gaussian curve, $\nu_{0,MAS}$ and $\Delta_i$ are the frequency with respect to $C_6F_6$ and the spinning rate of the sample, respectively. $A_{MAS}$, $B_{i,MAS}$ and $C_{MAS}$ are the intensities of the main peak, the spinning sideband and the base line, respectively. It is assumed that the left ($+\Delta_i$) and right ($-\Delta_i$) spinning sidebands have equal intensities to simplify the fitting.

### *Static NMR*

The sample was packed into a ϕ5.0 mm Pyrex glass tube in the static NMR measurements. The solid echo pulse sequence ($90^\circ_x$-$\tau$-$90^\circ_y$) was used, where $\tau$ was set at 7 μs. 32 echo signals were accumulated with a repetition time of 40 s. The spectra were fitted to the following Gaussian curve as a function of the frequency relative to $C_6F_6$:

$$f(\nu) = \frac{A_{SS}}{\beta_{SS}\sqrt{2\pi}}\exp\left[-\frac{(\nu-\nu_{0,SS})^2}{2\beta_{SS}^2}\right] + C_{SS} \qquad [2]$$

where $\beta_{SS}$ and $\nu_{0,SS}$ are the width between the centre and the inflection point of the Gaussian curve and the central frequency, respectively. $A_{SS}$ and $C_{SS}$ are intensities of the peak and the base line, respectively. As $CaF_2$ crystal has a small fourth moment, the NMR spectrum was fitted to Equation [3]**[15]**.

$$f(\nu) = A_{SS}\exp\left[-a^2(\nu-\nu_{0,SS})^2 - b^4(\nu-\nu_{0,SS})^4\right] + C_{SS} \qquad [3]$$

where $\nu_{0,SS}$ is the central frequency. $A_{SS}$ and $C_{SS}$ are intensities of the peak and the base line, respectively. *a* and *b* are constants.

## Results

### $^{19}F$ MAS NMR spectra

Figure 1 shows the $^{19}F$ NMR spectrum of cuspidine at the spinning rate of 10 kHz. Peaks with dots indicate spinning sidebands. Two sharp isotropic peaks are observed at 59.4 and 64.3 ppm and they have almost equal intensities. This result indicates that cuspidine has two inequivalent chemical states of fluorine with the same quantity. $CaF_2$ crystal has one broad peak at 58.6 ppm in good agreement with previous reports.**[16-18]**.

Table I shows the sample compositions determined by EPMA and the chemical shifts of $^{19}F$. Though the sample compositions are slightly changed by fluorine vaporization, these deviations are not critical to examine the chemical

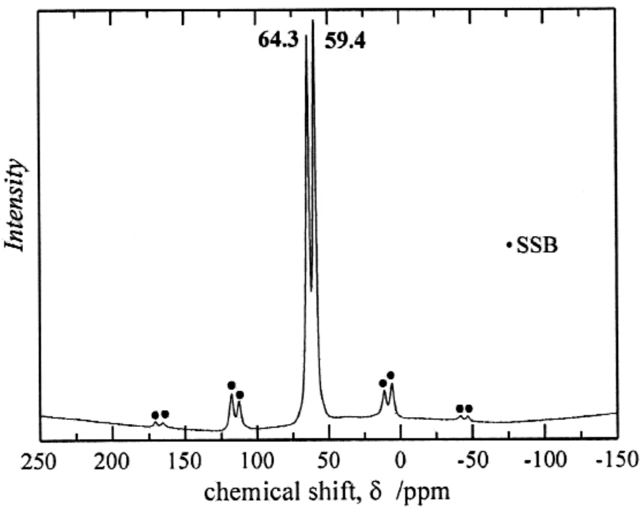

**Figure 1.** $^{19}$**F MAS NMR spectrum of cuspidine crystal at the spin rate of 10 kHz**

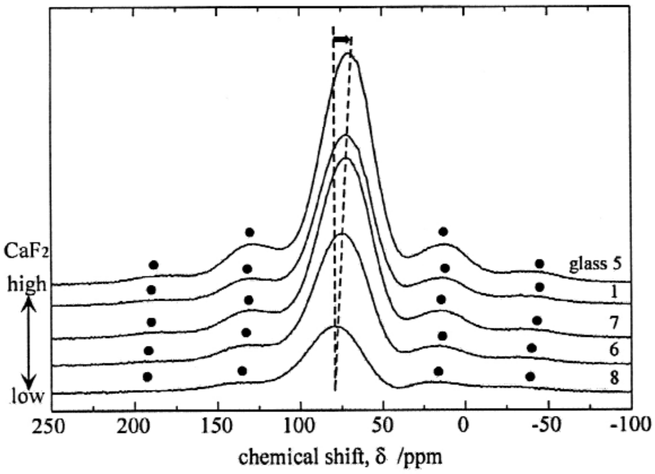

**Figure 2.** $^{19}$**F MAS NMR spectra of the SeriesI ((100-$x$)/2CaO-(100-$x$)/2SiO$_2$-$x$CaF$_2$ ) glasses at the spin rate of 10 kHz**

shifts. Figure 2 shows $^{19}$F MAS NMR spectra of Series I samples at the spinning rate of 10 kHz. The chemical shifts obviously decrease with increasing the CaF$_2$ content. Figure 3 shows spectra of Series II samples at the spinning rate of 10 kHz. Chemical shifts are decreased with increasing the CaF$_2$ content. Figure 4 shows spectra of Series III samples at the spinning rate of 10 kHz. The chemical shifts are constant irrespective of the CaO/SiO$_2$ ratio. In a basic glass (e.g. glass2), the NMR spectrum includes the peaks for cuspidine crystal, which crystallizes as a secondary phase on quenching.

Table II shows the fitting parameters, $\nu_{0,MAS}$ and $\beta_{MAS}$, of MAS NMR spectra. The parameter $\beta_{MAS}$ increases with increasing the CaF$_2$ content. Since there is no difference in the line width between the spinning rate of 10 and 12 kHz except for CaF$_2$ crystal, a spinning rate of 10 kHz is rapid enough to remove the contribution of $^{19}$F-$^{19}$F dipole-dipole interactions in these glasses.

### Static $^{19}$F NMR spectra

The fitting parameters, $\nu_{0,SS}$ and $\beta_{SS}$, of static NMR spectra are shown in Table II. The composition dependence of the $^{19}$F resonance frequency agrees with the case of MAS spectra. Each spectrum of the glasses is represented well by Equation [2]. Since the line shape of CaF$_2$ is campanulate, the spectrum is fitted by Equation [3].

## Discussion

### Chemical state of F in cuspidine crystal by MAS NMR

The crystal structure of cuspidine has been reported by Smirnova *et al.* and registered as 64710-ICSD.[19]. Figure 5 shows a schematic illustration of the unit cell of cuspidine. It consists of four units of Ca$_4$Si$_2$O$_7$F$_2$. There are two fluoride ions in the unit and each fluorine is coordinated with four calcium ions. The following values are the calculated Ca-F ionic distances based on the crystal structure:

Ca-F(1): 2.24, 2.25, 2.34, 2.39 Å
Ca-F(2): 2.28, 2.33, 2.36, 2.37 Å

These two fluorine atoms are not equivalent in terms of the Ca-F distances. The $^{19}$F NMR spectrum splitting shown in Figure 1 is consistent with the different average Ca-F distances between F(1) and F(2). Generally, the chemical shift depends on the ionic distances of the first nearest neighbours.[20]. The chemical shifts correspond to the average ionic distances as follows:

Average ionic distance: Ca-F(1,cuspidine)<Ca-F(2,cuspidine)<Ca-F(CaF$_2$ crystal)

**Table II**
**Fitting parameters $\beta_{MAS}$ and $\nu_{0,MAS}$ of MAS, $\beta_{SS}$ and $\nu_{0,SS}$ of static and second moment M$_2$ of $^{19}$F NMR spectra**

| | MAS | | static | | | | |
|---|---|---|---|---|---|---|---|
| | $\beta_{MAS}$ /Hz | $\nu_{0,MAS}$ /Hz | $\beta_{SS}$ /Hz | $\nu_{0,SS}$ /Hz | $\beta_{M2}$ /Hz | M$_2$ /Hz$_2$ | F concentration /Å$^{-3}$ |
| glass1 | 2800 | 13750 | 7580 | 14023 | 1.37_10$^4$ | 4.96_10$^7$ | 3.68_10$^{-3}$ |
| glass2 | 3000 | 13700 | 6730 | 13950 | 1.36_10$^4$ | 3.63_10$^7$ | 3.51_10$^{-3}$ |
| glass3 | 2800 | 13700 | 7800 | 14495 | 1.42_10$^4$ | 5.30_10$^7$ | 2.96_10$^{-3}$ |
| glass4 | 2950 | 13700 | 7600 | 14200 | 1.39_10$^4$ | 4.91_10$^7$ | 3.61_10$^{-3}$ |
| glass5 | 2950 | 12900 | 7980 | 13750 | 1.34_10$^4$ | 5.50_10$^7$ | 4.78_10$^{-3}$ |
| glass6 | 2950 | 14100 | 7300 | 14270 | 1.40_10$^4$ | 4.46_10$^7$ | 2.13_10$^{-3}$ |
| glass7 | 2950 | 13700 | 7580 | 13850 | 1.35_10$^4$ | 4.88_10$^7$ | 2.67_10$^{-3}$ |
| glass8 | 3100 | 14600 | 6400 | 14450 | 1.41_10$^4$ | 3.14_10$^7$ | 1.11_10$^{-3}$ |
| glass9 | 3200 | 14100 | 6400 | 14850 | 1.45_10$^4$ | 3.07_10$^7$ | 1.01_10$^{-3}$ |
| glass10 | 3000 | 13800 | 7350 | 14600 | 1.43_10$^4$ | 4.50_10$^7$ | 4.90_10$^{-4}$ |
| glass11 | 3000 | 13600 | 7570 | 14440 | 1.41_10$^4$ | 4.83_10$^7$ | 1.92_10$^{-3}$ |
| glass12 | 2800 | 13200 | 8330 | 14250 | 1.40_10$^4$ | 6.15_10$^7$ | 3.08_10$^{-3}$ |
| glass13 | 2800 | 13200 | 9000 | 13750 | 1.35_10$^4$ | 7.32_10$^7$ | 4.06_10$^{-3}$ |

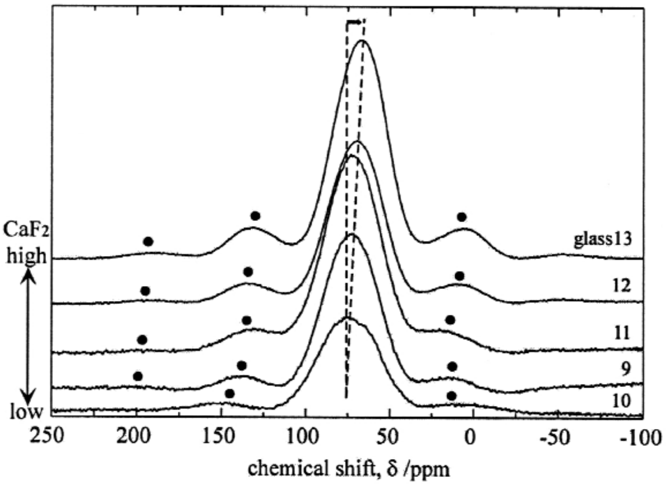

**Figure 3. $^{19}F$ MAS NMR spectra of the samples of SeriesII ((100-*x*)/3CaO-2(100-*x*)/3SiO$_2$-*x*CaF$_2$) at the spin rate of 10 kHz**

Chemical shift: $\delta_{F(1),cuspidine}(=64.3) > \delta_{F(2),cuspidine}(=59.4) > \delta_{F,CaF_2}(=58.6)$.

### Effect of fluorine on silicate-network in CaO-SiO$_2$-CaF$_2$ glasses

Figure 6 shows the sample composition and the chemical shift on the CaO-SiO$_2$-CaF$_2$ phase diagram in mass%. The chemical shift increases with decreasing the CaF$_2$ content, while it is constant irrespective of the CaO/SiO$_2$ ratio.

Duncan *et al.* investigated the $^{19}F$ NMR spectrum on the fluorine-doped silicate glass containing 1.03 mass%F. The glass was prepared by the modified chemical vapour deposition process.[21]. They measured the chemical shift and the distribution of nuclear dipolar couplings between fluorine nuclei by a spin echo method. They reported that isotropic chemical shift of Si(O$^-$)$_3$F was 24±1 ppm. The chemical shifts in the present study are closer to the value of the Ca-F bonding than that of the Si-F bonding. It is concluded that fluoride ions are coordinated with calcium ions in the composition range of the CaO-SiO$_2$-CaF$_2$ system.

Stebbins *et al.* performed $^{19}F$ MAS NMR of the 39.2mol%CaO-58.9mol%SiO$_2$-2.0mol%CaF$_2$ quenched glass at the spinning rate of 25 kHz and reported that the chemical shift of the sample was 79 ppm. The resonance shape and frequency of the $^{19}F$ NMR spectrum agree well with those values of the present study. However, they insisted that the Si-F-Ca bonding was present in molten slag and fluoride ions coordinated with silicon might move rapidly through the liquid and substitute for oxygen[13, 14].

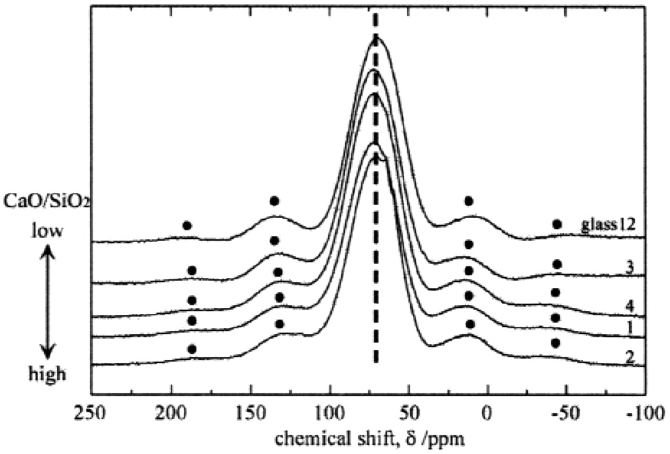

**Figure 4. $^{19}F$ MAS NMR spectra of the SeriesIII (*x*CaO-*y*SiO$_2$-15CaF$_2$) glasses at the spin rate of 10 kHz**

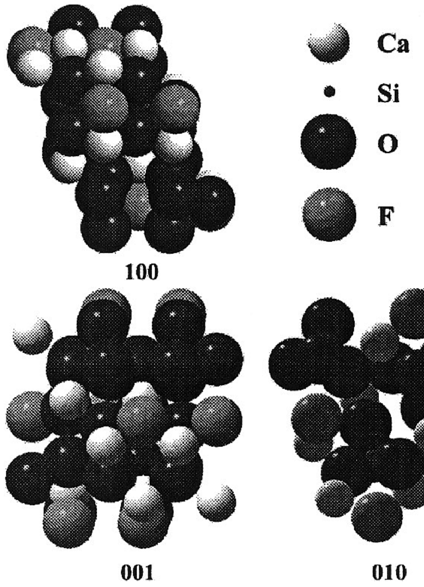

Symmetry space group: P1 21/c1
Symmetry cell setting: monoclinic
a= 7.55 Å
b= 10.43 Å
c= 10.85 Å
β= 69.93°

**Figure 5. Schematic illustration of unit cell of cuspidine (3CaO•SiO$_2$•CaF$_2$).**

Hayakawa *et al.* and Hayashi *et al.* have investigated the chemical states of fluorine and oxygen by X-ray photoelectron spectroscopy (XPS) on the CaO-SiO$_2$-CaF$_2$ quenched glass. Both of them reported the ratio of non-bonding oxygen (NBO) and total oxygen (BO+NBO)[10, 12]. Tsunawaki *et al.* also calculated the ratio NBO/(BO+NBO) by evaluating the Raman spectra[8]. In the *x*CaO-(1-*x*)SiO$_2$ glass, it is well accepted that BO/(BO+NBO) and NBO/(BO+NBO) can be expressed by the following equations:

$$\frac{BO}{BO+NBO}=\frac{2-3x}{2-x}=\frac{2-(CaO/SiO_2)}{2+(CaO/SiO_2)} \quad [4]$$

$$\frac{NBO}{BO+NBO}=\frac{2x}{2-x}=\frac{2(CaO/SiO_2)}{2+(CaO/SiO_2)} \quad [5]$$

Assuming that these values are also expressed as a function of the ratio of mol%CaO and mol%SiO$_2$ (=CaO/SiO$_2$), in case of *x*CaO-*y*SiO$_2$-(1-*x*-*y*)CaF$_2$ glasses, BO/(BO+NBO) and NBO/(BO+NBO) are expressed by the following equations:

$$\frac{NBO}{BO+NBO}=\frac{-x+2y}{x+2y}=\frac{2-(CaO/SiO_2)}{2+(CaO/SiO_2)} \quad [6]$$

$$\frac{NBO}{BO+NBO}=\frac{2x}{x+2y}=\frac{2(CaO/SiO_2)}{2+(CaO/SiO_2)} \quad [7]$$

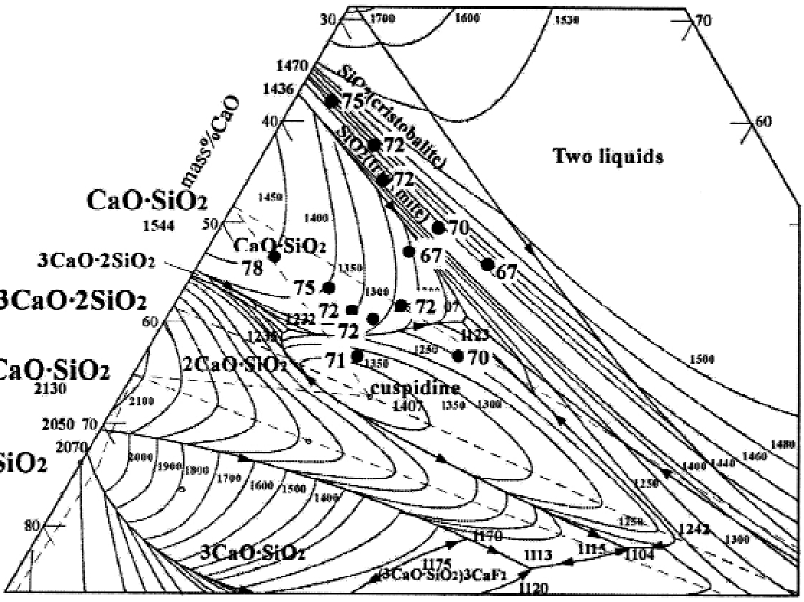

**Figure 6. Chemical shifts of $^{19}F$ with respect to $C_6F_6$ plotted on the phase diagram of $CaO$-$SiO_2$-$CaF_2$ system**

Figure 7 shows the relation between BO/(BO+NBO) and $CaO/SiO_2$. The solid line indicates the value calculated by Equation [6]. The observed BO/(NBO+BO) values are well described by Equation [6] and are dependent only on $CaO/SiO_2$. Moreover, the present result indicates that the chemical state of fluoride ions is not changed by $CaO/SiO_2$. As a consequence of these results, fluoride ion doesn't affect the polymerization of the silicate network in terms of the BO/NBO ratio.

### Chemical state of fluorine in $CaO$-$SiO_2$-$CaF_2$ glasses

$^{19}F$ static NMR spectral broadening is attributed to the distribution of the chemical state of F and $^{19}F$-$^{19}F$ dipole-dipole interactions. The fitting function, $f(\nu)$, is expressed as:

$$f(\nu) = \frac{A_{SS}}{\beta_{SS}\sqrt{2\pi}}\exp\left[-\frac{(\nu-\nu_{0,SS})^2}{2\beta_{SS}^2}\right] = \frac{A_{SS}}{\beta_{SS}\sqrt{2\pi}}\exp\left[-\frac{(\nu-\nu_{0,SS})^2}{2(\beta_{MAS}^2+\beta_{M2}^2)}\right] \quad [8]$$

Representing the NMR spectra by a Gaussian curve, the second moment of due to $^{19}F$-$^{19}F$ dipole-dipole interactions, $M_2$, corresponds to $\beta_{M2}^2$. The $\beta_{MAS}$ value is originated from the distribution of the F chemical state. Comparing the MAS and static NMR spectra, each $M_2$ value can be estimated by Equation [9]:

$$M_2 = \beta_{M2}^2 = \beta_{SS}^2 - \beta_{MAS}^2 \quad [9]$$

The second moment, $M_2$, is represented theoretically as follows[22]:

$$M_2 = <\Delta H^2> = \frac{3}{5}\gamma^4 h^2 I(I+1)\sum_{j,k} r_{jk}^{-6} \quad [10]$$

where $\gamma$ is the gyromagnetic ratio of fluorine (=$2.517\times10^4$ rad $G^{-1}$ $s^{-1}$), is Planck's constant (=$1.05457266\times10^{-34}$J s), $I$ is the spin quantum number (=1/2), $r_{jk}$ is a $^{19}F$-$^{19}F$ ionic distance in the sample. The $M_2$ value is a barometer of the spatial distribution of fluorine in the sample. The $M_2$ values of cuspidine and $CaF_2$ crystal can be calculated as $2.63\times10^7$ $Hz^2$ and $1.13\times10^8$ $Hz^2$ by Equation [10].

Table II shows the estimated $M_2$ of the glasses from the values of $\beta_{SS}$ and $\beta_{MAS}$. The $M_2$ of the glasses are plotted as a function of the square of the fluorine concentration in Figure 8. The $M_2$ of the glasses range over $3.1$–$7.3\times10^7$ $Hz^2$ and those are larger than the calculated value of cuspidine crystal.

A closed circle in Figure 8(a) shows the $M_2$ of powdered $CaF_2$ crystal. In $CaF_2$ crystal, fluoride ions form a simple cubic lattice. Assuming that fluoride ions in the glass distribute overall simple-cubic lattice points homogeneously, the $M_2$ value is proportional to the square of the fluorine concentration and its relation is presented by

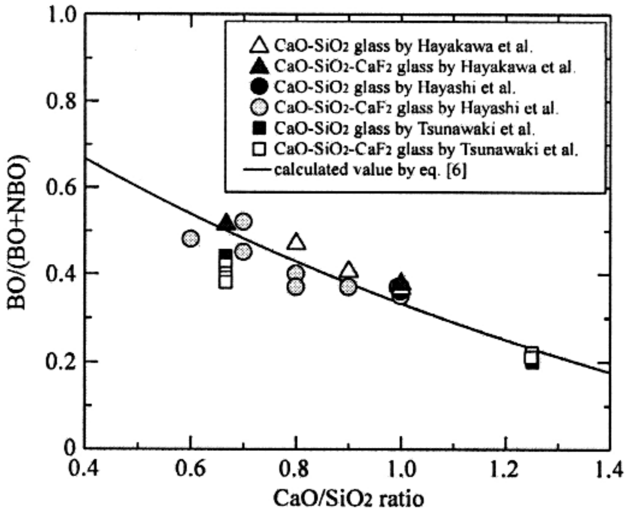

**Figure 7. BO/(BO+NBO) ratio as a function of $CaO/SiO_2$ ratio**

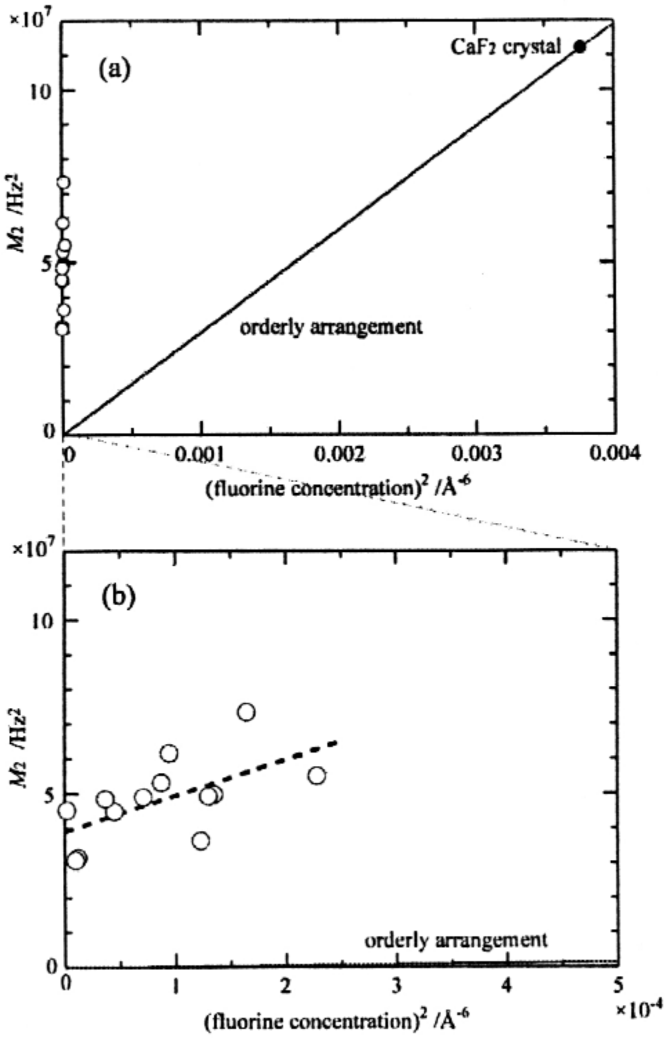

**Figure 8. (a) Relation between square of fluorine concentration and $^{19}F$ NMR second moment. (b) Magnified figure of low fluorine concentration region of (a)**

the solid line in Figure 8. In this case, the $M_2$ value is very small because of the large F-F distances. In the case where fluoride ions form Ca-F clusters in the glass, the $M_2$ value is much larger than in the former case. Furthermore, in the latter case, the $M_2$ value is strongly dependent on the Ca-F cluster size. Though the ionic distances increase with increasing the $CaF_2$ content, the $M_2$ values increase with increasing the $CaF_2$ content. Then, the Ca-F cluster size in the glasses grows with increasing the $CaF_2$ content.

Hayakawa *et al.* also calculated a structure of the 40mol%CaO-40mol%$SiO_2$-20mol%$CaF_2$ glass by molecular dynamics simulation (a MXDORTO system). They proposed a structure model of calcium oxyfluorosilicate glass. The glass consists of Si-O networks and Ca-F clusters[10]. The present results are consistent with the model that Hayakawa developed.

## Conclusion

Chemical states of fluorine in the CaO-$SiO_2$-$CaF_2$ glasses in the composition range of CaO/$SiO_2$ = 0.5–1.3 and 5–25 mol%$CaF_2$ have been investigated by $^{19}F$ solid-state NMR.

(i) The isotropic chemical shifts range from 67 to 78 ppm with respect to $C_6F_6$. In this composition range, the fluoride ion of the glasses is coordinated with less than four calcium ions and the ionic distance increases with an increase in the $CaF_2$ content.

(ii) The chemical state of fluoride ion, is independent of the degree of polymerization of the silicate network.

(iii) The NMR second moments of $^{19}F$-$^{19}F$ dipole-dipole interactions range from $3.1 \times 10^7$ to $7.3 \times 10^7$ $Hz^2$. They are larger than the vale of cuspidine crystal.

(iv) Fluoride ions form a Ca-F clusters. The size of Ca-F cluster increases with increasing the $CaF_2$ content.

## References

1. HANAO,M., KAWAMOTO,M., HARA,M., MURAKAMI, T., KIKUCHI,H. and HANAZAKI,K., Mold Flux for High Speed Continuous Casting of Hypoperitectic Steel Slabs, *Tetsu-to-Hagane*, vol. 88, 2002. pp. 23–28
2. WATANABE, T., FUKUYAMA, H. and NAGATA, K., Stability of Cuspidine ($3CaO•2SiO_2•CaF_2$) and Phase Relations in CaO-$SiO_2$-$CaF_2$ System, *ISIJ International*, vol. 42, no. 5, 2002. pp. 489–497
3. BÅÅK, T. and ÖLANDER, A., The System $CaSiO_3$-$CaF_2$, *Acta Chemica Scandinavica*, vol. 9, 1955. pp. 1350–1354.
4. BILLS, P.M., Viscosities in Silicate Slag Systems, *Journal of the Iron and Steel Institute*, 1963 pp. 133–140.
5. MITCHELL, A., Reactions of Calcium Silicates in Solution in Liquid Calcium Fluoride, *Transactions of Faraday Society*, vol. 63, 1967. pp. 1408–1417.
6. KUMAR, D., WARD, R.G. and WILLIAMS, D.J., Infra-red Absorption of Some Solid Silicates and Phosphates with and without Fluoride Additions, *Transactions of Faraday Society*, vol. 61, 1965. pp. 1850–1857.
7. IWAMOTO, N. and MAKINO, Y., A Structural Investigation of Calcium Fluorosilicate Glasses, *Journal of Non-Crystalline Solids*, vol. 46, 1981. pp. 81–94.
8. TSUNAWAKI, Y., IWAMOTO, N., HATTORI, T. and MITSUISHI, A., Analysis of CaO-$SiO_2$ and CaO-$SiO_2$-$CaF^2$ Glasses by Raman Spectroscopy, *Journal of Non-Crystalline Solids*, vol. 44, 1981. pp. 369–378.
9. ITO, H., YANAGASE, T., SUGINOSHITA, Y. and MIYAZAKI, N., Studies on the Structure of Molten Fluoride-Silicate Systems by Infrared Absorption Spectra, *Journal of the Japan Institute of Metals*, vol. 31, 1967. pp. 290–295.
10. HAYAKAWA, S., NAKAO, A. OHTSUKI, C., OSAKA, A., MATSUMOTO, S. and MIURA, Y., An x-ray photoelectron spectroscopic study of the chemical states of fluorine atoms in calcium silicate glasses, *Journal of Material Research*, vol. 13, 1998. pp. 739–743.
11. LUTH, R.W., Raman spectroscopic study of the solubility mechanisms of F in glasses in the system CaO-$CaF_2$-$SiO_2$, *American Mineralogist*, vol. 73, 1988. pp. 297–305.
12. HAYASHI, M., NABESHIMA, N., FUKUYAMA, H. and NAGATA, K., Effect of Fluorine on Silicate Network for CaO-$CaF_2$-$SiO_2$ and CaO-$CaF_2$-$SiO_2$-$FeO_x$ Glasses, *ISIJ International* vol. 42, no. 4, 2002. pp. 352–358.
13. STEBBINS, J.F. and ZENG, Q., Cation Ordering at Fluoride Sites in Silicate Glasses: a High-resolution $^{19}F$ NMR Study, *Journal of Non-Crystalline Solids*, vol. 262, 2000. pp. 1–5.

14. ZENG,Q. and STEBBINS, J.F., Fluoride Sites in Aluminosilicate Glasses: High-resolution $^{19}F$ NMR Results, *American Mineralogist*, vol. 85, 2000. pp. 863-867.

15. POWLES, J.G. and CRAZZA, B., A 'non-classical' information theory of spectral line shape, *Journal of Physics A Mathematical and General*, vol. 3, 1970. pp. 335–341.

16. KREINBRINK, A.T., SAZAVSKY, C.D., PYRZ, J.W., NELSON, D.G.A. and HONKONEN, R.S., Fast-Magic-Angle- Spinning $^{19}F$ NMR of Inorganic Fluorides and Fluoridated Apatitic Surfaces, *Journal of Magnetic Resonance*, vol. 88, 1990. pp. 267–276.

17. HARRIS, R.K., JACKSON, P. and NESBITT, G.J., Fluorine-19 CRAMPS and Its Application to the Solid-State Spectrum of Perfuluoronaphthalene, *Journal of Magnetic Resonance*, vol. 85, 1989. pp. 294–302.

18. SMITH, K.A. and BURUM, D.P., Application of Fluorine-19 CRMPS to the Analysis of Calcium Fluoride / Fluoroapatite Mixtures, *Journal of Magnetic Resonance*, vol. 84, 1989. pp. 85–94.

19. SMIRNOVA, R.F., MURANOVA, I.M. and BELOV, N.V., *Zapiski Vesoyuznogo Mineralogicheskogo Obshchestya*, vol. 84, 1955. pp. 159–169.

20. YAMAGATA, Y., Chemical shift, Relaxation Time, and Electric Quadrupole Coupling in Alkali Halides, *Journal of the Physical Society of Japan*, vol. 19, no. 1, 1964. pp. 10–23.

21. DUNCAN, T.M., DOUGLASS, D.C., CSENCSITS, R. and WALKER, K.L., Study of fluorine in silicate glass with $^{19}F$ nuclear magnetic resonance spectroscopy, *Journal of Applied Physics*, vol. 60, no. 1, 1986. pp. 130–136.

22. VAN VLECK, J.H., The Dipolar Broadening of Magnetic Resonance Lines in Crystal, *Physical Review*, vol. 74, no. 9, 1948. pp. 1168–1183.